Torsion Balance for Measurement of Capillary Immersion Forces

Ceco D. Dushkin,*,† Peter A. Kralchevsky,† Vesselin N. Paunov,†
Hideyuki Yoshimura,‡ and Kuniaki Nagayama‡

Laboratory of Thermodynamics and Physico-chemical Hydrodynamics, Faculty of Chemistry, University of Sofia, 1126 Sofia, Bulgaria, and Protein Array Project, ERATO, JRDC, 5-9-1 Tokodai, Tsukuba 300-26, Japan

Received July 10, 1995. In Final Form: October 6, 1995⊗

Particle−particle and particle−wall capillary interactions were measured as a function of the separation distance. The "particles" were vertical thin glass cylinders and/or small glass spheres, protruding from an air/liquid interface. The particles attract each other due to the overlapping of the menisci formed around each of them. The force of interaction is detected by a sensitive torsion microbalance. It is based on counterbalancing the moment of a couple of forces, acting between two pairs of particles, by the torsion moment of a thin platinum wire. By varying the wire diameter, we accessed forces differing by several orders of magnitude, from about 5 dyn at small separation between the particles down to 0.001 dyn at large separation. The smallest force was measured with two cylinders of diameters about 300 μm. For two spheres (diameters 1.2 mm) we obtained difference in the forces corresponding to different heights of protrusion from the liquid surface. For interacting sphere and glass cylinder the force follows similar trends as the forces between two spheres or two cylinders. In the case of sphere and glass wall, however, the force first increases with decreasing the distance and then decreases close to the wall passing through a maximum. The predictions of the theory of capillary immersion forces are in quantitative agreement with the experimental results.

1. Introduction

For a long time capillary forces were believed to play an important role in the interaction between colloidal particles attached to a liquid interface.[1] This importance was stressed recently in connection with the formation of two-dimensional arrays of fine particles.[2] It was observed experimentally that, despite of their size (micrometer,[3] submicrometer,[4] or nanometer[5]), the particles confined in a thin suspension film on a substrate form an ordered monolayer due to a sort of long range lateral attractive force (capillary force). This force arises in the course of thinning the suspension film down to a thickness of less than the particle diameter[3,6] when the particles protrude from the liquid−air interface. The cause of the lateral capillary forces is the deformation of the liquid surface around the particle which allowed theoretical computation of the force by solving the Laplace equation of capillarity in relevant geometry (for a review see ref 7). The forces acting on particles partially immersed in a wetting liquid film on a substrate, called immersion capillary forces, should be distinguished from the flotation capillary forces acting on particles floating freely on a liquid interface. The origin of the flotation forces is the particle weight causing a deformation of the liquid surface whereas the immersion forces are related to the wetting properties of the particle surface rather than to gravity.[7] The immersion forces, being much stronger due to their origin, can be significant even for nanometer size particles compared to the flotation forces which practically vanish for particles smaller in size than 10 μm. Here we consider forces acting among particles constrained on a liquid−air interface which are a sort of capillary immersion forces.

As shown theoretically[8,9] the capillary interaction between two spherical particles can be successfully approximated by the interaction between two vertical cylinders used recently for experimental determination of the capillary forces.[10] The force balance developed in ref 10 allowed measurement of the force between two glass capillaries immersed in liquid: one of them attached to a stepper motor gradually approaches the other one attached to the sensitive core of a pressure transducer. The force was determined from the transducer output voltage plotted on chart recorder versus the separation distance. For a couple of capillaries of diameters 740 and 630 μm the measured force ranged from about 0.1 to 4 dyn depending on the separation distance. At one and the same distance the force measured for pure water was roughly twice the force obtained for surfactant solution which could be explained simply by twice larger surface tension in the former case than in the latter, in agreement with the theoretical predictions.[8,9]

Despite of the experimental work[10] there are questions which still remain open:

(i) About the force between spherical particles which are much closer in shape to the real colloidal particles than the model cylinders. There is only one attempt[11] to measure the force between two spheres attached to a water−oil interface in an oil film spread on water. Unfortunately, the experimental data obtained in ref 11 could not be quantitatively interpreted by means of the

* Author for correspondence
† University of Sofia.
‡ Protein Array Project.
⊗ Abstract published in *Advance ACS Abstracts,* December 15, 1995.

(1) Nicolson, M. M. *Proc. Cambridge Philos. Soc.* **1949**, *45*, 288.
(2) Denkov, N. D.; Velev, O. D.; Kralchevsky, P. A.; Ivanov, I. B.; Yoshimura, H.; Nagayama, K. *Nature (London)* **1993**, *361*, 26.
(3) Denkov, N. D.; Velev, O. D.; Kralchevsky, P. A.; Ivanov, I. B.; Yoshimura, H.; Nagayama, K. *Langmuir* **1992**, *8*, 3183.
(4) Dushkin, C. D.; Yoshimura, H.; Nagayama, K. *Chem. Phys. Lett.* **1993**, *204*, 455.
(5) Nagayama, K. *Materials Sci. Eng.* **1994**, *C1*, 87.
(6) Dimitrov, A. S.; Dushkin, C. D.; Yoshimura, H.; Nagayama, K. *Langmuir* **1994**, *10*, 432.
(7) Kralchevsky, P. A.; Nagayama, K. *Langmuir* **1994**, *10*, 23.
(8) Kralchevsky, P. A.; Paunov, V. N.; Ivanov, I. B.; Nagayama, K. *J. Colloid Interface Sci.* **1992**, *151*, 79.
(9) Kralchevsky, P. A.; Paunov, V. N.; Denkov, N. D.; Ivanov, I. B.; Nagayama, K. *J. Colloid Interface Sci.* **1993**, *155*, 420.
(10) Velev, O. D.; Denkov, N. D.; Paunov, V. N.; Kralchevsky, P. A.; Nagayama, K. *Langmuir* **1993**, *9*, 3702.
(11) Camoin, C.; Roussell, J. F.; Faure, R.; Blanc, R. *Europhys. Lett.* **1987**, *3*, 449.

0743-7463/96/2412-0641$12.00/0

theory of capillary forces[8,9] because important experimental parameters (surface tension, contact angle) were not determined. Capillary interaction between two spherical particles is studied experimentally also in the case of liquid bridges existing between two particles placed in another fluid, e.g. in air.[12,13] However, the nature of these forces, directed *normally* to the plane of the contact line, is quite different from the *lateral* capillary immersion forces investigated by us.

(ii) About the magnitude of the capillary force acting between much smaller particles than the ones used in refs 10 and 11. Following the analogy between spheres and cylinders, the results from ref 10 can be related with the interaction between spherical particles of diameter about 1 mm. At the same time the particles in real colloidal systems are typically of much smaller size (about 1−10 μm or less) which will lead to vanishingly smaller capillary forces. Although it seems hard to measure such small forces now, any lowering of the particle size could be important for understanding the nature of these forces as well as for proving theoretical assumptions.

To clarify points i and ii we carried out new experiments with particles of appreciably smaller size than the ones described in literature.[10,11] The smaller size implies smaller forces. For this purpose we utilized a new technique based on the classical torsion balances for gravitational and electrostatic forces[14] (for a recent review of the problem see ref 15). In this case there are two couples of interacting particles: two of the particles are attached to an anchor suspended on a metal wire, whereas the other two particles are attached to holders. Approaching each other synchronously, the particles create a couple of forces leading to a force moment, which is then counterbalanced by the torsion moment of the wire. As model particles in a couple, we used two glass cylinders (diameters 730 or 330 μm), two spheres (diameters 1.2 mm), a sphere and cylinder, or a sphere and a plate, mimicking solid wall. The particles are situated at a certain distance apart on the surface of a liquid phase, either water or water−surfactant solution. By varying the diameter of the metal wire, we accessed forces differing by several orders of magnitude, from about 5 dyn to less than 0.001 dyn, with the lower limit much smaller than the magnitude of capillary forces measured until now.[10,11] The experimental data reported here are well described by the theory for capillary immersion forces.

2. Operation Principle of the Torsion Balance

2.1. Calculation of the Force. Here we give a brief outline of the principle of operation of a torsion balance[14] and its application of our special torsion balance for measurement of capillary forces. Let us consider two particles, 1′ and 1″, attached to an anchor of arm *a* shown in Figure 1a. The anchor suspended on a fine wire can rotate around a vertical axis coinciding with the wire. The other two particles, 2′ and 2″, are attached to holders in a way to form two couples with the anchor particles. To create a couple of equal forces particles 1′ and 1″, as well as particles 2′ and 2″, should be identical. Experimentally the distance between the centers of particles in a couple is maintained $L' = L'' = L$ corresponding to a force $F(L)$. We adjust the force perpendicular to the anchor arm by adapting the position of the holders (Figure 1b). Thus a moment $Fa/2$ with respect to the anchor center is

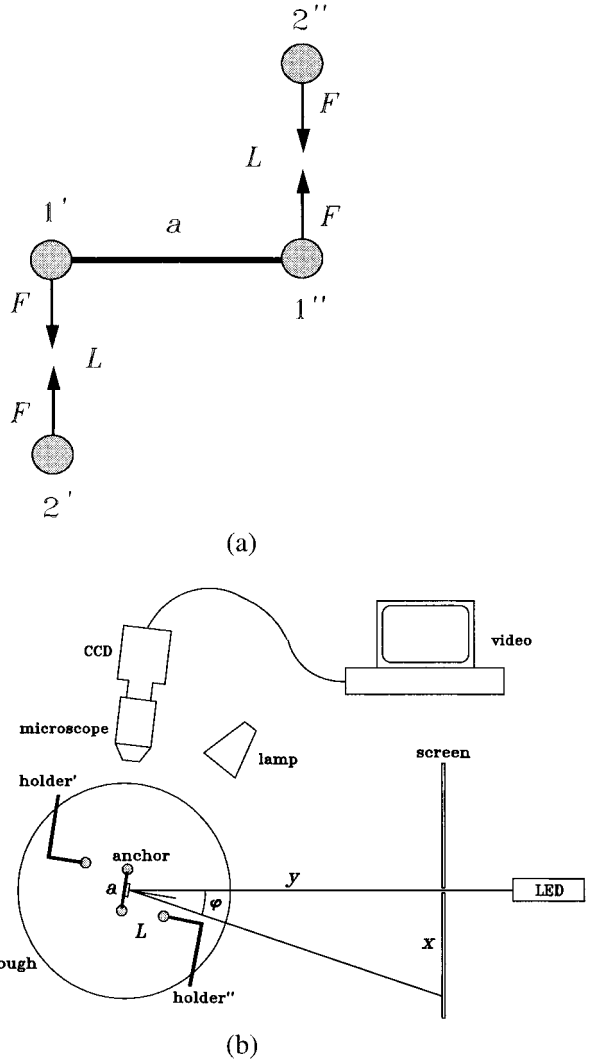

Figure 1. Scheme of the experimental setup for measuring capillary forces between particles immersed in liquid medium: (a) forces between two couples of interacting particles; (b) top view demonstrating the principle of measurement.

created, so that the total moment of the couple of forces is

$$M = Fa \tag{2.1}$$

At equilibrium this moment is counterbalanced by the torsion moment of the wire

$$M = f\varphi_0 = f\frac{\varphi}{2} \tag{2.2}$$

where f is the torsion modulus; $\varphi_0 = \varphi/2$ is the angle of torsion (in rad) which is equal to half of the total angle of reflection of the light φ measured experimentally (see Figure 1b). By equating (2.1) and (2.2), one obtains

$$F = f\varphi/2a \tag{2.3}$$

For cylindrical wire f is given by[14]

$$f(l) = \pi G\delta^4/2l \tag{2.4}$$

where δ is the wire radius, l is the wire length, and G is the elastic modulus of the wire material. Combining eqs 2.3 and 2.4, one can obtain the force by measuring experimentally f and φ (see below).

2.2. Determination of the Torsion Modulus. One can follow a classical procedure[14] of measuring the period

(12) Mason, G.; Clark, W. C. *Chem. Eng. Sci.* **1965**, *20*, 859.
(13) Gillespie, T.; Settineri, W. J. *J. Colloid Interface Sci.* **1967**, *24*, 199.
(14) Sivuhin, D. V. *General Course of Physics*; GRFML: Moscow, 1979 (in Russian).
(15) Gillies, G. T.; Ritter, R. C. *Rev. Sci. Instrum.* **1993**, *64*, 283.

of oscillations T of a solid body of known inertia moment I suspended on the wire

$$T = 2\pi\sqrt{\frac{I}{f}} \tag{2.5}$$

Substituting (2.4) into (2.5) one obtains for the period of oscillations

$$T(l) = \beta\sqrt{l} \tag{2.6}$$

where

$$\beta = \frac{2}{\delta^2}\sqrt{\frac{2\pi I}{G}} \tag{2.7}$$

is a constant. It is seen from eq 2.6 that T should depend linearly on $l^{1/2}$.

For a cylinder of mass m_c and radius R_c the inertia moment is

$$I_c = \frac{1}{2}m_c R_c^{\,2} \tag{2.8}$$

It follows from eqs 2.5 and 2.8 that in this case

$$f = 2\pi^2 \frac{m_c R_c^{\,2}}{T^2} \tag{2.9}$$

Knowing the period of oscillations, T, one can calculate the torsion modulus f from eq 2.9 for any wire length l. In view of eq 2.4 f should be a linear function of $1/l$

$$f = K\frac{1}{l} \tag{2.10}$$

where

$$K = \frac{\pi G}{2}\delta^4 \tag{2.11}$$

is a torsion coefficient determined experimentally. Once the torsion modulus f is calculated, one can use it to obtain the force by eq 2.3.

3. Experimental Setup

Figure 1b represents a view from above the experimental setup with the constituting parts of the balance: anchor and holders with interacting particles (solid circles). The mirror attached to the anchor reflects the light beam coming from the red light emitting diode (LED). The screen placed between the light source and the balance is to measure the angle, φ, of light reflection from the mirror. The distance y between the aperture pierced in the screen center and the anchor mirror is always kept constant and equal to 40 cm. The light beam passing through the aperture is reflected by the mirror and returned back to the screen to form a light spot of mean diameter about 1−2 mm. We calculated the angle of reflection φ by measuring the distance x from the aperture to the center of this light spot:

$$\varphi = \arctan\frac{x}{y} \tag{3.1}$$

The torsion balance shown in Figure 2 consists of an anchor with two particles attached (1) suspended on a thin platinum wire (2), mechanism for manipulating the wire (3−9), frame (10−12), base (13−16), two holders for attaching the other two particles (17), and a liquid trough (18). To vary the range of forces accessible experimentally, we use combinations of anchors of different size and weight (Table 1) and platinum wires of different diameters: 25 and 100 μm (Table 2). The wire is wound on a reel (3) which can be rotated by the screw (5) and be fixed at a given

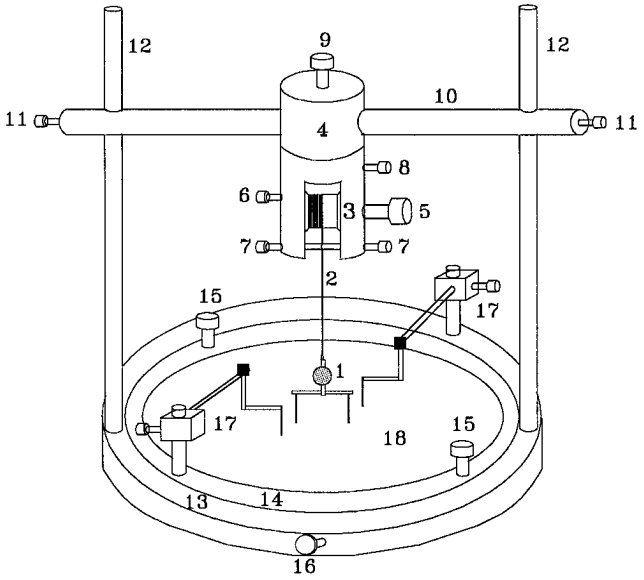

Figure 2. Scheme of the torsion microbalance for measuring the lateral immersion force (for notations see the text).

Table 1. Anchors Used To Measure Capillary Forces

	anchor 1	anchor 2
mass, m (g)	0.136	8.921
length, a (cm)	1.0	2.8
inertia moment, I_a (g·cm^2)	$8.5 \times 10^{-3} \pm 1.2 \times 10^{-4}$	1.74 ± 0.07

Table 2. Platinum Wires Used To Measure Capillary Forces

	25 μm wire[a]	100 μm wire[b]
radius, δ (μm)	12.5	50.0
maximum overload, m_{max} (g)	0.62	9.98
torsion coefficient, K (dyn·cm^2)	2.03085	589.48553
elastic modulus, G (dyn/cm^2)	5.296×10^{11}	6.005×10^{11}

[a] Wire strength measured by suspending cylinder 1. [b] Wire strength measured by suspending cylinder 2.

position by another screw (6). In this way one can vary the wire length l, i.e. the torsion modulus $f(l)$; cf. eq 2.10. To fix the wire length and prevent any lateral motion, the wire is pressed between two screws (7). At fixed wire length the anchor can be centered with respect to the liquid through and to the light beam by horizontal motion of the wire holder along the rod (10) and by vertical motion along two vertical rods (12). In this manner one can vary the distance between the anchor and the liquid surface and, hence, the depth of immersion of particles 1′ and 1″ in the liquid without changing the wire length. The anchor can rotate around the vertical axis due to special connection between the lower and upper part (4) of the wire holder (the two parts can be fixed by the screw (8)).

The other two particles, 2′ and 2″, are attached to the holders (17) on the ring (14) which can rotate around the anchor and be fixed to the base by two screws (15). The construction of the holders allows movement of the attached particles in vertical and horizontal directions as well as tilting them in order to adjust the distance L between the particles in a couple and the depth of immersion.

All parts of the torsion balance considered above are made of stainless steel. The liquid trough (18) is a glass Petri dish of inner diameter 9 cm fixed to the balance by the screws (16). The upper part of the dish is a Teflon ring which has with water a contact angle close to 90°, thus providing a flat interface suitable for our measurements. The total height of the balance is about 20 cm, and at the outer diameter of the base the height is about 11 cm.

The balance is placed on the table of vertical optical microscope (Nikon), not depicted in Figure 1b. In this way the whole balance (together with the liquid trough) can be moved in two horizontal directions in order to center precisely the anchor with respect to

Table 3. Brass Cylinders for Calibration of the Torsion Moments of Platinum Wires

	cylinder 1[a]	cylinder 2[b]
radius, R_c (cm)	0.40	0.75
length, L_c (cm)	0.41	2.00
mass, m_c (g)	1.698	29.933
inertia moment, I_c (g·cm^2)	0.135	8.486
β_c (s/cm$^{1/2}$)	1.6186	0.8035

[a] Cylinder suspended on wire ∅25. [b] Cylinder suspended on wire ∅100.

the light beam. This microscope allows also optical observation of the particles from below in transmitted light when necessary. A horizontal optical microscope (Zeiss) is used to observe the meniscus profile around the particles in reflected light. The optical image from this microscope is monitored on a TV screen and recorded by SVHS system (Sony).

We utilized two types of anchors: a smaller anchor (anchor 1), always suspended on 25 μm platinum wire, and a bigger anchor (anchor 2), suspended on 100 μm wire (Table 1). Anchor 1 consists of two cylindrical rods, horizontal rod and vertical, connected perpendicularly to each other. The axis of symmetry of the vertical rod passes through the middle of the horizontal rod. On the vertical rod a glass mirror is mounted with its reflection surface parallel to the axis of rotation. The mirror is so small (diameter 3.2 mm; mass 0.009 g) that it cannot affect appreciably the inertia moment of the anchor. Anchor 1 is attached tightly to the platinum wire by special conical fitting.

To measure cylinder−cylinder interaction, we attached at the two ends of the horizontal rod two glass capillaries of equal diameters about 330 μm at a distance between the glass capillaries $a = 1.0$ cm. Much thinner capillaries of diameter 100 μm can also be used with this anchor.[16] To attach spherical particles of diameter 1.2 mm, we used auxiliary glass capillaries of diameter about 300 μm. Each glass sphere was glued at the capillary tip by means of epoxiresine (Bison). The auxiliary capillaries were bent in a way allowing the sphere to protrude from below from the liuqid surface. The distance between the two spheres was $a = 3.9$ cm. Similar was the construction of the glass capillaries with spheres which are attached to the holders.

Anchor 2 consists of a metal cylinder with two symmetrical arms and platinum wire attached to the upper face of the cylinder. To study cylinder−cylinder interaction, we glued two glass capillaries of equal diameters 730 μm to the arms at a distance between the capillaries of $a = 2.8$ cm. For interactions between spheres, two auxiliary bent glass capillaries bearing 1.2 mm spherical particles were attached directly to the metal cylinder. The distance between the two spheres on the anchor was $a = 3.0$ cm.

For interactions including spheres (sphere−sphere, sphere−cylinder, or sphere−plate), the spheres were always attached to the anchor whereas the respective counterparts (spheres, cylinders, or plates) were glued to the holders.

Anchor 1 is too light to be suspended on 100 μm wire whereas 25 μm wire is too thin to resist the weight of anchor 2. We calculated the maximum load

$$m_{max} = \pi\delta^2 p_{max}$$

which can be applied to a wire, from the limit of stretching rigidness of platinum ($p_{max} = 1.27 \times 10^{-3}$ g/μm^2).[17] As seen from Table 2 the mass of anchor 2 is close to m_{max} for wire ∅25.

4. Experimental Procedures

4.1. Materials. We used cylinders (capillaries), spheres, and plates, all of them made of glass. The capillaries of diameters 320 and 340 μm were home made whereas the capillaries of diameter 730 μm were prepared from microsyringe pipets of volume 2 μL (Sigma). The total length of a capillary was about 1.5−2 cm. We used two sets of glass spheres of close mean diameter 1200 μm.

(16) Dushkin, C. D.; Yoshimura, H.; Nagayama, K. Submitted for publication in *J. Colloid Interface Sci.*

(17) Hampel, C. A., Ed. *Rare Metals Handbook*; Chapman and Hall: London, 1961.

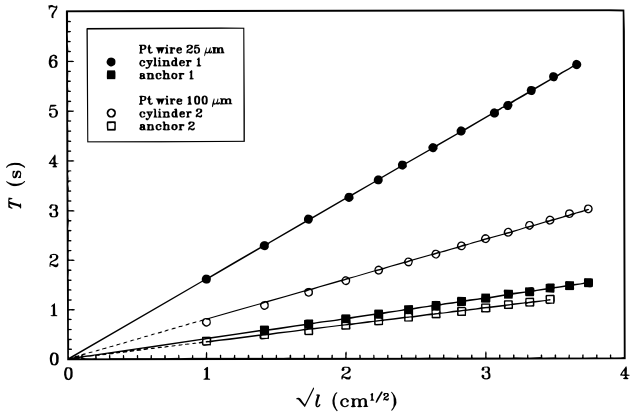

Figure 3. Periods of oscillations T of standard cylinders and anchors suspended on platinum wires of different diameters and different length l. The solid lines are the best fits of the experimental data by eq 2.6.

The interaction between sphere and a wall was simulated by attaching a microcover glass plate of dimensions 18 × 18 × 0.15 mm (Matsunami) to each holder.

The glass capillaries and plates were washed with chromic acid and distilled water prior to attachment to the holders. It was also possible to clean their lower parts immersed in the liquid before each measurement. However, the glass spheres were washed only with distilled water prior to the measurement since the chromic acid destroyed the epoxiresine.

The liquid phase was either deionized water (Millipore) or water solution of sodium dodecyl sulfate, SDS (Fluka), with concentration 8×10^{-2} mol/L, same as the concentration utilized in ref 10. The high surfactant concentration assures constancy of the surface tension throughout one experiment (which may continue several hours), as well as zero contact angle with the glass surfaces.

4.2. Determination of Torsion Modulus. The wire torsion modulus was determined by measuring the period of oscillations of a standard brass cylinder suspended on the wire in air. We utilized two types of cylinders: smaller cylinder (cylinder 1), always suspended on 25 μm platinum wire, and a bigger cylinder (cylinder 1), suspended on 100 μm wire (Table 3). Cylinder 1 consists of two hemicylindrical parts which can be disassembled to press the wire end between them. In this way very thin wires, e.g. 25 μm or less,[16] can be adjusted exactly in the cylinder center. The 100 μm wire was glued in the center of cylinder 2. We varied the period of oscillations by changing the wire length. The oscillations, provoked by carefully turning the cylinder to a certain initial angle, were counted with the use of a horizontal optical microscope. The total time t for a series of ten oscillations was measured with accuracy 0.01 s; hence, the period of oscillation is $T = t/10$. Though the amplitude of subsequent oscillations in one series decayed with time due to friction with the air, the period of oscillation remained always constant, as it should be.

Figure 3 plots the period of oscillations T versus square root of the wire length l. Each point is a mean value of 5−10 independent experiments. The standard deviation of the data is too small to be shown in the figure because of the very good reproducibility of T. It is seen that according to eq 2.6 the period of oscillation of a *cylinder* is a linear function of $l^{1/2}$. The smaller cylinder oscillates faster than the bigger one since it is of lower mass, i.e. lower inertia moment I_c, and is suspended moreover on platinum wire of lesser strength (cf. eq 2.5).

Similar experiments were done also for the free oscillations of the *anchors* suspended on the respective wires.

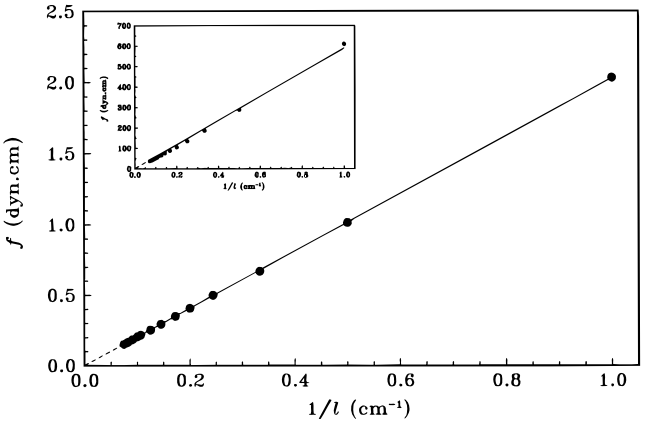

Figure 4. Torsion modulus f of platinum wire of diameter 25 μm vs the reverse wire length. The solid line is the best fit of the experimental data by eq 2.10. The inset shows the same plot for platinum wire of diameter 100 μm.

In this case the period T was measured by following the motion of the light spot reflected from the mirror. As for the cylinders, there is also a good linearity between T and $l^{1/2}$ (Figure 3) from where we calculated the anchor inertia moment I_a. The anchors oscillate faster since they have much smaller inertia moments than the respective metal cylinders (Tables 1 and 3). These data agree well with the respective values obtained by calculating I_a from the anchor geometry using known theorems.

Figure 4 shows that the torsion modulus f, calculated by eq 2.9 from the data in Figure 3, depends linearly on the reverse wire length $1/l$ (cf. eq 2.10). Knowing the values of the torsion constant K, we estimated the elastic moduli of the platinum wires (Table 2), which are very close to the values reported in literature:[18] $G = 5.884 \times 10^{11}$ to 7.1×10^{11} dyn/cm^2. The same values can be obtained also by eq 2.7 if the constant β_c is calculated from the slopes of the curves in Figure 3.

4.3. Measurement of the Force. First we poured liquid in the trough (ca. 40 mL) up to the upper edge of the Teflon ring. The thickness of the liquid layer was about 7 mm. After that we adjusted the wire length by winding the reel and pressing the wire. Then we leveled the wire holder to immerse the anchor particles in the liquid. The immersion depth for glass cylinders is about 3 mm for their lower edge. The spheres were first totally immersed in the liquid and then the anchor was carefully moved up until the particles protrude symmetrically from the liquid surface. We adjusted the anchor mirror perpendicular to the incident beam by rotating the wire holder around the vertical axis. This position corresponds to zero interaction. The next step was to immerse the holder particles in the liquid. For spheres we adjusted their height of protrusion the same as the height of protrusion of the anchor spheres. The distance L between the particles in a couple was then varied by slowly moving the holders along the liquid surface. This distance was measured with an accuracy of 10 μm either directly by an electronic calliper gauge (Mitutoyo) or from the TV monitor.

After one of the holder particles was moved, the anchor rotates to angle φ'. When the second particle is moved, this angle increases with φ''. Hence, the total angle of rotation is $\varphi_0 = \varphi' + \varphi''$. Knowing the angle $\varphi_0 = \varphi/2$, one can calculate the force by means of eq 2.3. In the ideal case of uniform response of the two couples, $\varphi' = \varphi'' = \varphi/4$, which allows measurement of the force by only one couple

(18) *Landolt-Börnstein Physikalisch Chemische Tabellen*; Springer: Berlin, 1923; p 80.

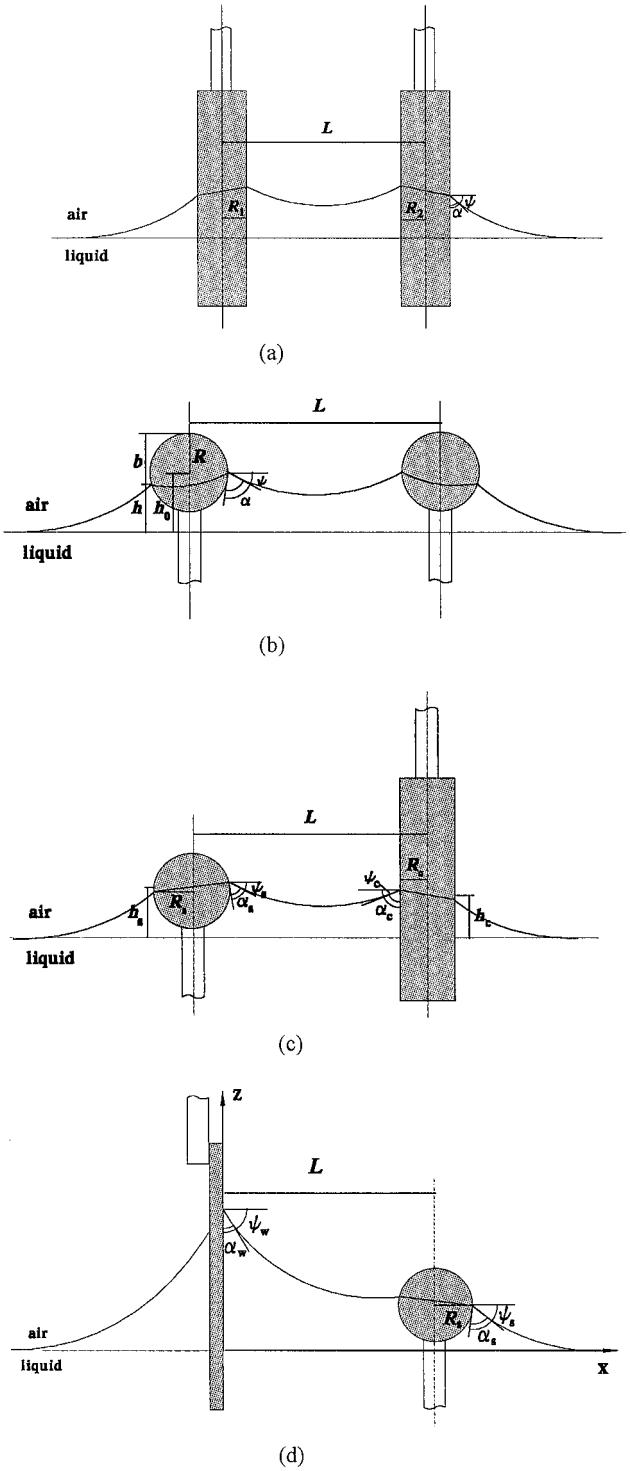

Figure 5. Sketch of a couple of two interacting particles and the surrounding meniscus: (a) cylinder−cylinder; (b) sphere−sphere; (c) sphere−cylinder; (d) sphere−wall.

of particles. To test this possibility, we approached one of the holder capillaries alone to the respective anchor capillary and found that $\varphi' \approx \varphi''$ at one and the same distance L. On the basis of these results we carried out two types of measurements: (i) measurement of the force F acting between the particles in the two couples together as in most of the experiments on cylinder−cylinder and sphere−sphere interaction; (ii) measurement of the force F acting at a distance L between the particles in one of the couples alone. The experiments on sphere−cylinder and sphere−wall interactions belong to this type because it was difficult to equally adjust and to record the two couples simultaneously. For spheres of close protrusion,

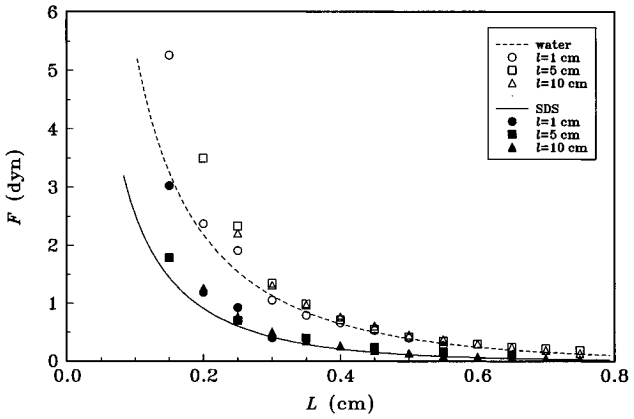

Figure 6. Capillary force F versus the distance L between two interacting glass cylinders of equal radii $R_1 = R_2 = 0.0365$ cm. The cylinders are immersed either in pure water ($\sigma = 72.4$ dyn/cm, $q = 3.681$ cm^{-1}) or in SDS solution ($\sigma = 36.8$ dyn/cm, $q = 5.163$ cm^{-1}). The force is measured by anchor 2 suspended on 100 μm platinum wire at different wire length l. The theoretical curves are drawn according to eq 6.1 without any adjustable parameters.

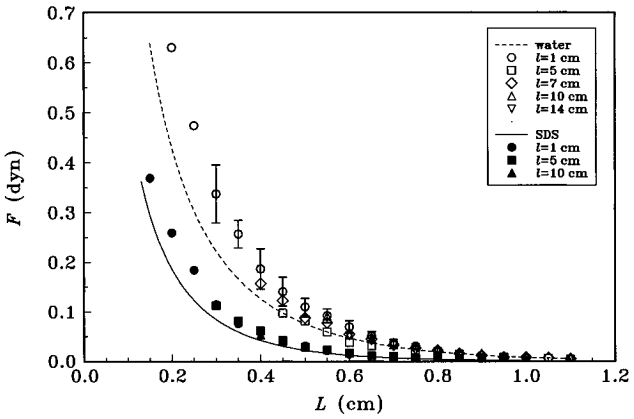

Figure 7. Capillary force F versus the distance L between two interacting glass cylinders of radii $R_1 = 0.016$ cm and $R_2 = 0.017$ cm immersed either in pure water or in SDS solution. The force is measured by anchor 1 suspended on 25 μm platinum wire at different wire length l. Theoretical curves are drawn according to eq 6.1 without any adjustable parameters.

$F' \approx F'' = F$ within the experimental error, which makes these experiments quite reasonable.

For pure water the liquid surface was cleaned prior to the experiment by sucking out some liquid from the surface with a syringe. The force measurements were completed within 30 min to 1 h from the cleaning in order to diminish the effect of contamination of the water surface. Very important for calculation of the capillary force is the contact angle between the liquid meniscus and the capillary wall. Although this angle is almost zero with water, it can vary slightly due to contamination on the water or glass surfaces. In the experiments with SDS solution the force measurement started at least 30 min after the surfactant solution was poured in the trough to establish equilibrium surface tension $\sigma = 36.8$ dyn/cm.[10]

The experimental error of a single force measurement (not larger than 5%) was determined chiefly by the accuracy of the angle φ, i.e. of the distance x on the screen (cf. eq 3.1). Other possible sources of uncertainty can be any interaction with the more distinct particle on the anchor or nonperpendicular location of the holder particles with respect to the anchor. Our calculations showed that both effects can lead to no more than 7% difference between the force F measured experimentally and the actual capillary force F_c.

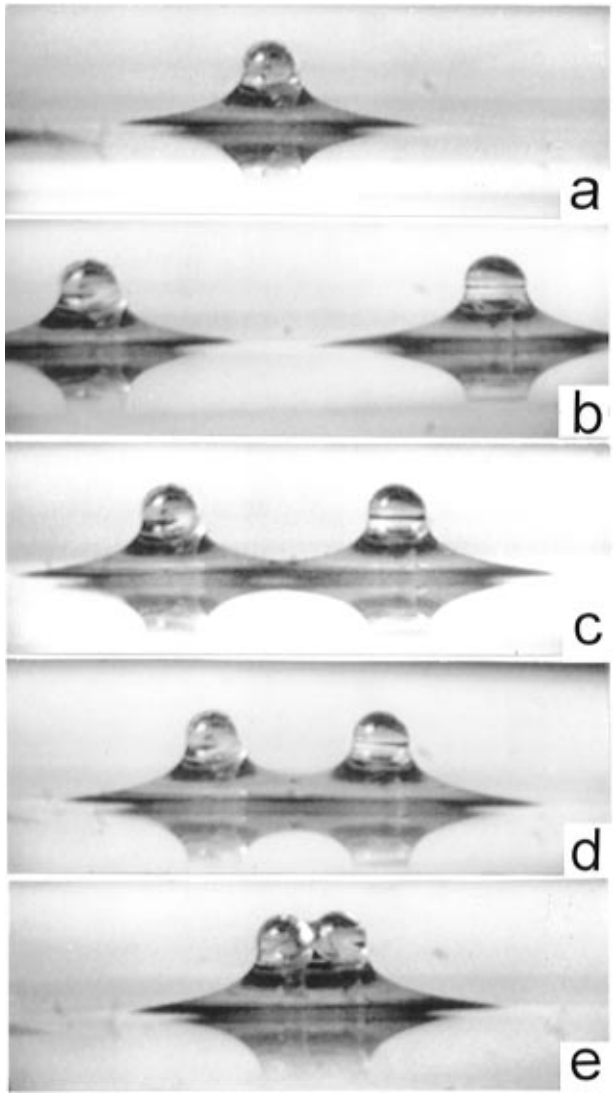

Figure 8. Successive stages of interaction of two glass spheres of diameters 1.2 mm immersed in SDS solution at protrusion height $h_\infty = 1.05$ mm. The left sphere is attached to anchor 2 suspended on platinum wire of diameter 100 μm and length 10 cm. The right sphere is attached to the holder. The measured forces are as follows: (a) $L = \infty$, $F = 0$; (b) $L = 0.854$ cm, $F = 0.074$ dyn; (c) $L = 0.479$ cm, $F = 0.442$ dyn; (d) $L = 0.353$ cm, $F = 1.129$ dyn; (e) $L = 1.2$ mm, $F = \infty$.

All measurements were carried out at room temperature 20−23 °C.

5. Experimental Results

5.1. Force of Interaction between Two Vertical Cylinders (Figure 5a). The force between glass capillaries of equal diameters, 730 μm, is shown in Figure 6. Each set of figures corresponds to a fixed wire length l. For certain interparticle distance, L the forces obtained at different wire length coincide within the experimental accuracy. For pure water (empty figures) the force is about two times larger than the force for SDS solution (solid figures) because the surface tension of water is twice larger (cf. eq 6.1 below). Since the force increases appreciably when the cylinders come close to each other, larger forces are measured by using shorter wire of higher torsion strength. At a distance less than 2 mm the force becomes so strong that it overcomes the wire strength and the capillaries spontaneously stick to each other.

The force acting between glass capillaries of two times smaller diameters than those in Figure 6 is plotted vs L

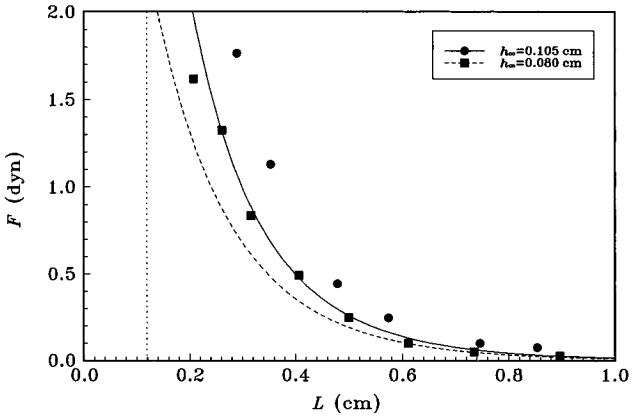

Figure 9. Dependence of the capillary force F on the distance L between two glass spheres of uniform diameter 1.2 mm immersed in SDS solution. The platinum wire is of diameter 100 μm and length 10 cm. Each set of data corresponds to different protrusion height h_∞. The curves are plotted by means of eq 6.1 at different contact angles. The dotted vertical line corresponds to the closest approach.

in Figure 7. The error bars for $l = 1$ cm are the standard deviations from three successive measurements of the force. The larger the force, the large the uncertainty of its detection since the anchor becomes unstable at small separations, close to the point of spontaneous sticking of capillaries. Again, forces obtained at different wire length coincide within the experimental accuracy and the force for pure water is appreciably larger than the force for SDS solution. In general, the forces in Figure 7 are about 10 times lower than the respective forces for twice larger capillaries in Figure 6. Although the force is weaker in the former case, the maximum distance for detection of any force is longer ($L \sim 1.2$ cm) because the sensitivity of 25 μm platinum wire is much higher than that of 100 μm wire.

5.2. Force of Interaction between Two Spheres (Figure 5b). Figure 8 represents photographs of two glass spheres located on the liquid surface at different separation distances, L. At infinite separation (single sphere in Figure 8a) the meniscus is symmetrical and the three-phase contact line at the particle surface is horizontal. The meniscus is leveling off to the horizontal water surface far from the sphere. One can expect appreciable force when the two spheres come close to each other at a distance of the order of the capillary length q^{-1} defined by eq 6.3 below, since the range of capillary interactions is determined by q^{-1} (for SDS solution $q^{-1} = 0.194$ cm). Figure 8b is at separation of minimum detectable force with 100 μm platinum wire (with 25 μm wire we extended this limit up to 1.3 cm). When the separation distance is decreased, the force becomes larger since the menisci overlapping is stronger (Figure 8c). At very close separation ($L \leq 2q^{-1}$) the overlap is so strong that the inclination of the contact line, which is the reason for the lateral capillary forces, becomes visible (Figures 8d). Finally, the two spheres stick to each other, Figure 8e, because the force exceeds the torsion strength of the wire. The photographs taken at smaller protrusion of the sphere tops (with respect to the level of the nondisturbed liquid surface) showed that the larger protrusion, the steeper the liquid meniscus surrounding the particles.

When the height of protrusion decreases, the capillary force should also decrease because the extend of the menisci diminishes. This is supported by Figure 9 comparing the forces measured at two different protrusion heights: $h_\infty = 1.05$ mm shown in Figure 8 and $h_\infty = 0.8$ mm. It is clearly seen that in the latter case (boxes) the force is always smaller than the force in the former case (circles).

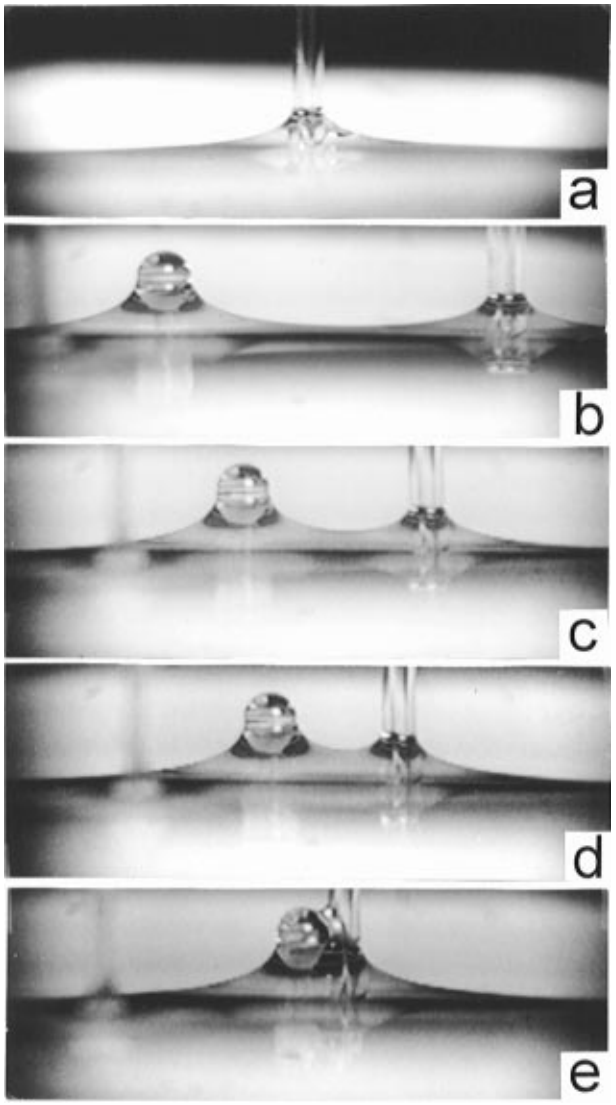

Figure 10. Successive stages of interaction of a glass sphere of diameter 1.2 mm and glass cylinder of diameter 0.73 mm immersed partially in solution of SDS. The protrusion height of the sphere is $h_\infty = 1.2$ mm and of the cylinder is $h_c = 0.95$ mm (the other parameters are the same as in Figure 8). The measured forces are as follows: (a) $L = \infty$, $F = 0$; (b) $L = 0.897$ cm, $F = 0.025$ dyn; (c) $L = 0.5$ cm, $F = 0.246$ dyn; (d) $L = 0.406$ cm, $F = 0.491$ dyn; (e) $L = 0.965$ mm, $F = \infty$.

5.3. Force of Interaction between Sphere and Cylinder or Glass Wall (Figure 6c,d). Photographs of a partially immersed glass sphere and a glass cylinder approaching each other are shown in Figure 10. The measured force, plotted vs L in Figure 11, follows a similar trend as for two spheres or two cylinders.

The photographs in Figure 12 are side views of a partially immersed glass sphere and a glass plate (solid wall) approaching each other. The perturbation created by the wall extends to a larger distance than the respective perturbations created by the cylinder (cf. Figure 10) or the sphere (Figure 8). This means stronger interaction between the sphere and the wall leading to larger force plotted in Figure 13. Each set of data was obtained by one couple of particles. The sphere approaches the middle of the wall perpendicularly to its surface. The experimental data for the force in Figure 13 exhibit maximum near the wall surface due to the fact that at $L < 0.1$ cm the sphere is immersed deeper in the meniscus on the

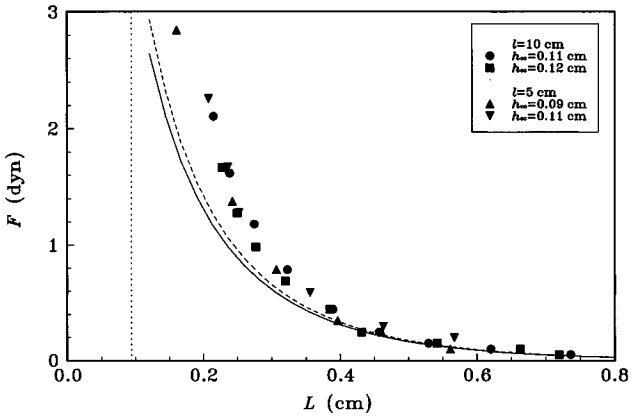

Figure 11. Dependence of the capillary force F on the distance L between a glass sphere of diameter 1.2 mm and a glass cylinder of diameter 0.73 mm immersed in SDS solution. Each set of data is obtained by one couple of particles. The platinum wire is of diameter 100 μm and different length l. The height of sphere protrusion h_∞ varies between 0.9 and 1.2 mm. The vertical dotted line corresponds to the closest approach.

wall (Figure 12e,f). Consequently, the contact line shrinks, thus decreasing the force of interaction.

6. Discussion

6.1. Comparison with Other Experiments. First we compare our results for the capillary force between the larger cylinders of radii 365 μm with the experimental data from ref 10 obtained with two different cylinders of radii 315 and 370 μm. Our data are in good agreement with the data of the other authors[10] (see Figure 14) although the cylinder diameters are not exactly the same. Nevertheless, one should emphasize the difference in the operational principle and construction of the two force balances, which can lead to difference in their applicability. The basic difference in sensitivity comes from the detection system: we measure the force by the torsion of a metal wire whereas in ref 10 the force is detected by pressure transducer. By decreasing the wire diameter, we can decrease sufficiently the lower limit of forces accessible with our balance. For example, with Pt wire of diameter 10 μm, torsion constant $K \approx 0.05$ dyn·cm^2, and length $l \approx 10$ cm one can detect in principle forces down to about 10^{-4} dyn (10^{-9} N).[16]

One cannot compare quantitatively our data for the capillary force between two spheres with the data of Camoin et al.[11] because, as mentioned above, neither the size or the spheres nor the liquid interface utilized by these authors are close to our system. Moreover, important experimental features of their system like the interfacial tension three-phase contact angle, and the radii of the contact lines are unknown. Bearing in mind the magnitude of the forces detected by them, it seems that our torsion balance is of better sensitivity than the balance described in ref 11. Moreover, in our experiment the spherical particles protrude from below from the liquid−air interface in contrast to their system where the particles enter the interface from above. One can expect that the attachment of a spherical particle to a fiber can lead to some change in the wetting properties of the sphere surface in the vicinity of contact. Hence, entering the liquid interface from the air side as in ref 11 is less convenient, especially for small spherical particles and small protrusion heights.

6.2. Comparison of Theory and Experiment: Cylinder−Cylinder Interaction. The predictions of linear theory for the capillary force between two cylinders[7−9] is in quantitative agreement with our experimental

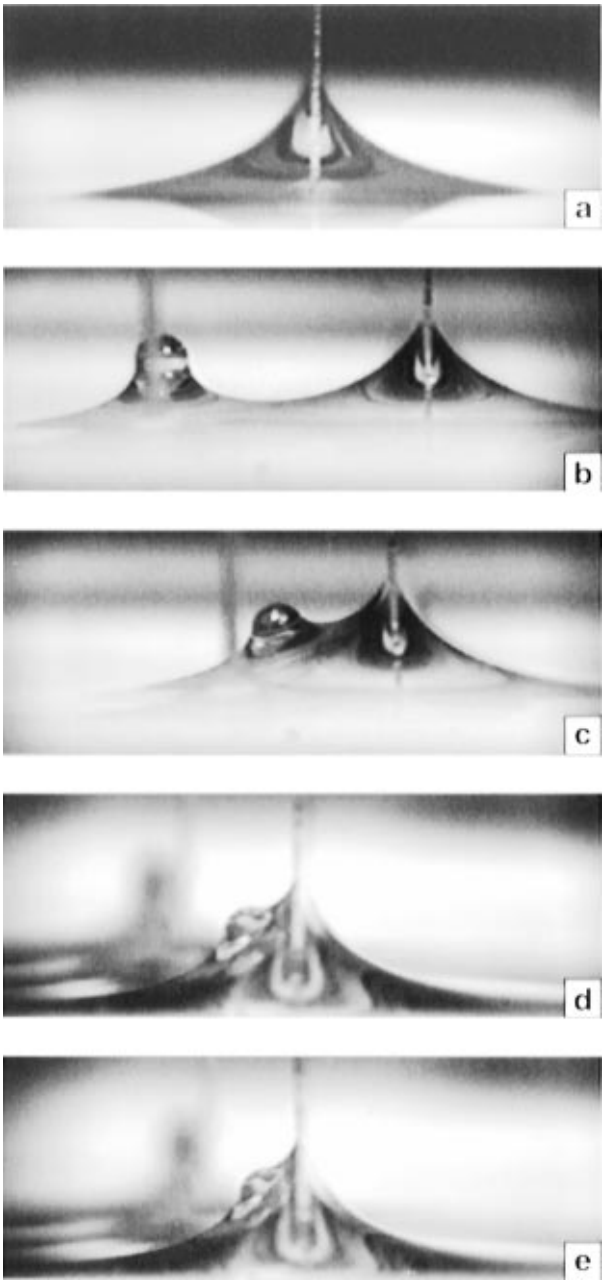

Figure 12. Successive stages of interaction of a glass sphere of diameter 1.2 mm and a vertical glass plate immersed in solution of SDS. The protrusion height of the sphere is $h_\infty = 1.15$ mm and of the wall is $h_w = 2.1$ mm. The platinum wire has diameter 100 μm and length 5 cm. The measured forces are as follows: (a) $L = \infty$, $F = 0$; (b) $L = 0.472$ cm, $F = 1.277$ dyn; (c) $L = 0.236$ cm, $F = 4.693$ dyn; (d) $L = 0.113$ cm, $F = 6.331$ dyn; (e) $L = 0.084$ cm, $F = 5.466$ dyn.

data plotted in Figures 6 and 7 (see the respective curves). According to this theory the capillary force acting between two cylinders, 1 and 2, immersed partially in a liquid is given by the equation

$$F = 2\pi\sigma q Q_1 Q_2 K_1(qL) \tag{6.1}$$

Here σ is the surface tension of the liquid; Q_i is the so-called capillary charge

$$Q_i = R_i \sin \psi_i, \qquad i = 1, 2 \tag{6.2}$$

where ψ_i is the meniscus slope angle at the particle contact line (Figure 5a); K_1 is the modified Bessel function of second kind, first order; and

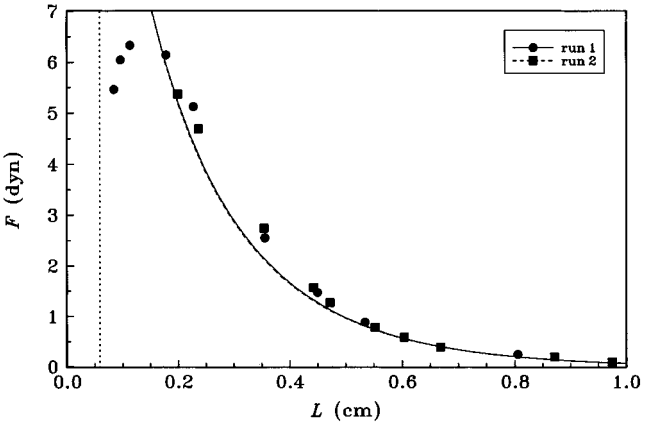

Figure 13. Dependence of the capillary force F on the distance L between glass sphere of diameter 1.2 mm and glass plate immersed in SDS solution. The platinum wire is of diameter 100 μm and length $l = 5$ cm. The two sets of data are obtained by two runs with one couple of particles. In both cases the height of sphere protrusion is $h_\infty \approx 1.05$ mm. The solid and dashed curves are calculated by theory without usage of any adjustable parameters. The vertical dotted line corresponds to the closest approach.

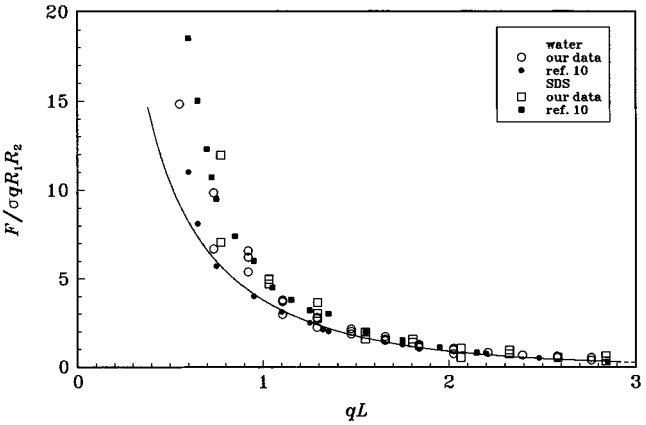

Figure 14. Comparison of the capillary force measured in our experiment between two interacting glass cylinders of equal radii $R_1 = R_2 = 0.0365$ cm with data from ref 10 for glass cylinders of close radii, $R_1 = 0.0315$ cm and $R_2 = 0.037$ cm. Our data (the empty figures) are the same as in Figure 6. The theoretical curve is drawn according to eq 6.1 with the cylinder radii values 0.0365 cm.

$$q = \sqrt{\frac{\Delta\rho g}{\sigma}} \tag{6.3}$$

is the reverse capillary length, where g is the acceleration due to gravity and $\Delta\rho$ is the density difference between liquid and air (in our experiments $\Delta\rho = 1$ g/cm^3). Equation 6.1 is derived assuming small meniscus slope over the entire fluid surface and thin cylinders, i.e. $\sin^2\psi \ll 1$. The capillary length q^{-1} can be considered as a decay length of the lateral capillary force because at large values of the distance L, $K_1(qL)$ decays roughly exponentially with decay length q^{-1}.

Since the contact angle at the *cylinder* wall is kept nearly zero in our experiments, the slope angle will be $\psi_i \cong \pi/2$ ($\sin\psi_i \cong 1$), which allows replacement of Q_i in eq 6.1 simply by R_i. The theoretical curves in Figures 6 and 7 are drawn according to this equation without any adjustable parameter. It is seen that the theory agrees fairly well with the experiment especially at large separations ($L > q^{-1}$). The discrepancy between the linear theory and experiment at small separations ($L \sim q^{-1}$) appears because the assumptions made when deriving eq 6.1 are no longer valid. To describe the force in this case one should solve numerically and nonlinearized Laplace equation of capillarity. The thinner the cylinders, the closer the linear theory and the experiment. This is confirmed also for much thinner cylinders.[16]

Capillary Interaction between Two Spheres. As for two cylinders, the lateral capillary force between two spherical particles is given by eq 6.1[8,9] where Q_i is determined by

$$Q_i = r_i \sin\psi_i, \qquad i = 1, 2 \tag{6.4}$$

In eq 6.4 r_i is the radius of the contact line given by

$$r_i = R_i \sin(\alpha + \psi_i) \tag{6.5}$$

where α is the contact angle and R_i is the sphere radius. Since the spherical particles in our experiments are of very close radii, $2R_1 = 0.1179$ cm and $2R_2 = 0.1199$ cm, we considered for simplicity two similar particles of one and the same radius $R = (R_1R_2)^{1/2} = 0.05945$ cm. Then $\psi_1 = \psi_2 = \psi$ and $r_1 = r_2 = r$.

By variation of the distance between the particles, L, the slope angle ψ in eq 6.5 and the contact line radius $r(L)$ also vary. At a given value of the elevation of the particle center, h_0, and contact angle, α, we calculated the values of the geometrical parameters r, b, h, and ψ, determining the particle position by using eq 6.5 and the following three equations[8,9]

$$b = R[1 - \cos(\alpha + \psi)] \tag{6.6}$$

$$h(L) = Q \ln\frac{4}{\gamma_e qr(1 + \cos\psi)} + QK_0(qL) \tag{6.7}$$

$$h_0 = h(L) + b(L) - R \tag{6.8}$$

where γ_e (=1.78...) is the number of Euler−Masceroni, K_0 is the modified Bessel function of zeroth order, and b and h are mean values taken along the contact line[8,9] (for definition see Figure 5b). Solving the set of equations (6.4−6.8) we obtained the dependence $Q(L)$ and then calculated the lateral capillary force from eq 6.1.

Since the particles are of fixed vertical position, the height h_0 remains the same as for the single sphere without capillary interaction

$$h_0 = h_\infty + b_\infty - R \tag{6.9}$$

($L \to \infty$, cf. Figure 8a) where

$$b_\infty = R[1 - \cos(\alpha + \psi_\infty)] \tag{6.10}$$

$$h_\infty = Q_\infty \ln\frac{4}{\gamma_e qr_\infty(1 + \cos\psi_\infty)} \tag{6.11}$$

$$r_\infty = R\sin(\alpha + \psi_\infty) \tag{6.12}$$

Equation 6.11 was derived by Derjaguin[19] long ago.

To determine the contact angle, α, the following experimental values of the parameters were used: $b_\infty = 0.073$ cm for $h_\infty = 0.105$ cm (circles) and $b_\infty = 0.045$ cm for $h_\infty = 0.08$ cm (squares); see Figure 9. Then we calculated by eqs 6.9−6.12 particle contact angles $\alpha = 16°$ and $\alpha = 23°$, respectively. Since for one and the same couple of particles α should be constant, we attributed this difference in α to the experimental error in measuring b_∞ and h_∞. We proved numerically that small differences in b_∞ and h_∞ within the experimental error can lead to significant

(19) Derjaguin, B. *Dokl. Akad. Nauk USSR* **1946**, *51*, 517.

deviations in the calculated α up to $\pm 6°$. In spite of this inaccuracy we processed further the experimental data for the force by the asymptotic expression (6.1). The results are given in Figure 9 by the solid curve for $b_\infty = 0.073$ cm and by the dashed curve for $b_\infty = 0.045$ cm. The theory describes well the measured force at comparatively large distances ($qL \gg 1$); however, at short distances eq 6.1 underestimates the capillary force. This discrepancy between the linear theory and the experiment is due to the large meniscus slope around the particles as well as to their large radii compared to the capillary length q^{-1}. Better coincidence with the experiment can be achieved only by solving the nonlinear Laplace equation of capillarity.

Capillary Interaction between Cylinder and Sphere. For the capillary force acting between vertical cylinder of radius R_c and a spherical particle of radius R_s (Figure 5c) we used again the approximate expression (6.1). The only difference with respect to the case of two spheres is that the capillary charge of the cylinder does not depend on L (cf. eq 6.2). The procedure of calculating the capillary charge of the sphere is the same as described in the previous subsection where eq 6.7 should be replaced with

$$h_s(L) = Q_s \ln \frac{4}{\gamma_e q r_s (1 + \cos \psi_s)} + Q_c K_0(qL) \qquad (6.13)$$

(the subscripts "s" and "c" refer to the sphere and the cylinder, respectively). Equation 6.13 is derived by using superposition approximation for the meniscus shape which is valid even for large meniscus slope around the particles, but only at large interparticle distances.[10]

The experimental runs in Figure 11 correspond to various vertical positions of the spherical particle defined by h_∞ and three-phase contact angle at the cylinder wall $\alpha_c = 0°$. The contact angle of the spherical particle α_s was determined from b_∞ and h_∞ as described for two interacting spheres. Knowing the capillary charge of the cylinder, $Q_c = R_c = 0.0365$ cm, we calculated the capillary force by eq 6.1. The theoretical curves practically coincide because the geometrical parameters for the different runs are close to each other. The linear theory and the experiment agree well at large separations L whereas the discrepancy at small L is due again to nonlinear effects.

Capillary Interaction between Sphere and Wall. For a spherical particle of radius R protruding from the liquid surface at a distance L from a vertical planar wall (Figure 6d) the three-phase contact angles at the wall and the sphere are α_w and α_s, respectively. The lateral capillary force between floating spherical particle and a wall is given by the approximate expression[20]

$$F(L) \approx \pi\sigma[2qQ_s^2 K_1(qL) + 2Q_s \tan \psi_w e^{-qL/2} + q(r_s \tan \psi_w e^{qL/2})^2] \qquad (6.14)$$

valid at small meniscus slope and relatively large distances, $L \gg r_c$. The difference between the particle floating on the liquid surface and the particle fixed in vertical direction is just in the expression for Q_s. Below we generalize eq 6.14 for the case of large meniscus slopes around the particle and the wall and large distance L compared with the capillary length q^{-1}.

It is known, that far from a single wall the meniscus shape decays exponentially,[10]

$$z(L) = \frac{1}{q} D e^{-qL}, \qquad qL \gg 1 \qquad (6.15)$$

where

$$D = 4\left(\tan \frac{\psi_w}{4}\right) \exp\left(-4 \sin^2 \frac{\psi_w}{4}\right)$$

At small meniscus slope angle at the wall ψ_w eq 6.15 reduces simply to

$$z(L) = \frac{1}{q} \tan \psi_w e^{-qL} \qquad (6.16)$$

which is used when deriving (6.14). By using eq 6.15 instead of 6.16, one can derive a counterpart of eq 6.14, viz.

$$F(L) \approx -\pi\sigma[2qQ_s^2 K_1(qL) + 2Q_s D e^{-qL/2} + q(r_s D e^{-qL/2})^2] \qquad (6.17)$$

which is valid for large meniscus slope and large particle−wall separations. The dependence of Q_s on L is calculated as described for two spheres where eq 6.7 is replaced with its counterpart

$$h_s(L) = \frac{1}{q} D e^{-qL} + Q_s \ln \frac{4}{\gamma_e q r_s (1 + \cos \psi_s)} + Q_s K_0(qL) \qquad (6.18)$$

It is worth noting that the above equations describe well the magnitude of the measured capillary force only at large separations ($qL \geq 1$).

The prediction of eq 6.17 and the experimental data for the capillary force between glass plate and a sphere are seen in Figure 13. The contact angle at the sphere wall α_s was calculated as described previously for a single sphere at $\alpha_w = 0$. The results presented by solid curve ($b_\infty = 0.064$ cm) and dashed curve ($b_\infty = 0.070$ cm) practically coincide. At small distances the approximate expression cannot predict the experimentally observed maximum of the force; most probably this effect can be described again by the exact solution of the nonlinear Laplace equation.

7. Conclusions

The main results of our experimental study on capillary forces can be summarized as follows:

(i) We measured capillary forces between particles immersed partially in liquid by a special version of the classical torsion microbalance constructed by us (Figures 1 and 2). Two of the particles are attached to an anchor suspended on a platinum wire, whereas the other two particles are attached to holders synchronously approaching the anchor. By varying the wire strength and type of the anchor, we can detect forces from several dynes to <1 mdyn, which allows us to access very small capillary forces. Using this balance, we measured the capillary attraction between two glass cylinders, two spheres, a sphere and cylinder, and a sphere and wall immersed partially either in pure water or in surfactant solution; see Figure 5.

(ii) The experimental results for two cylinders of diameters 730 μm are in good agreement with data for a similar system obtained by another type of force balance[10] (Figure 14). For linear theory for capillary forces agrees quantitatively with the data especially at not too small separations between the particles (Figure 6). The agreement is much better for cylinders of diameters about twice as small (320−340 μm), even at small separations (Figure 7). At one and the same separation the force for pure

(20) Kralchevsky, P. A.; Paunov, V. N.; Denkov, N. D.; Nagayama, K. *J. Colloid Interface Sci.* **1994**, *167*, 47.

(21) Velev, O. D.; Denkov, N. D.; Paunov, V. N.; Kralchevsky, P. A.; Nagayama, K. *J. Colloid Interface Sci.* **1994**, *167*, 66.

water is about twice larger than the force for surfactant solution which comes from the difference in the surface tension.

(iii) For two spheres of diameters 1.2 mm we measured the force at different heights of protrusion of a sphere from the liquid surface and found that at larger protrusion the force is also larger. The linear theory predicts the force well at large separation between the spheres and fails at close separation due to nonlinear effects (Figure 9).

(iv) We measured also the capillary force between sphere and glass cylinder and between sphere and glass wall. While in the first case the force exhibits similar trends as the force between two spheres or two cylinders (Figure 11), in the second case the force first increases with decreasing the distance and then decreases passing through a maximum (Figure 13).

We hope that these experimental findings can be useful for understanding the capillary interaction between colloidal particles and protein macromolecules. As mentioned above, such forces play a role for the aggregation of particles in two-dimensional arrays on substrate.[3−5]

Acknowledgment. This work was supported by the Research and Development Corporation of Japan (JRDC) under the program Exploratory Research for Advanced Technology (ERATO). The precise manufacturing of the torsion microbalance by the Japanese company Sanyu is greatly acknowledged.

LA950560P